(Online) ISSN 2712-0562
Original Research

Sustainable Engineering and Innovation
Vol. 8, No. 2, 2026, pp.17-38
https://doi.org/10.37868/sei.v8i2.id1024

Designing and manufacturing a solar heater similar to a cake mold (CM)

Rusul Dawood Salim[1], Wasan L. AL-Salim[2*], Mazin Jawad Kadhim[3], Jassim M. AL-Asadi[4]
[1,4] Department of Physics, College of Education for Pure Science, University of Basra, Basrah, Iraq
[2] Southern Technical University, Basra Technical Institute, Basrah, Iraq
[3] Basrah Oil Company, Production Department, Iraq

*Corresponding author E-mail: wasan.loay@stu.edu.iq

Received Jan. 17, 2026
Revised May 2, 2026
Accepted Jul 3, 2026
Online Aug. 13, 2026

Abstract

This study presents the design, fabrication, and experimental evaluation of a novel, low-cost solar water heater utilizing a compact cake mold (CM) geometry. The configuration enhances solar absorption by increasing the heat-transfer pipe's effective length. The system integrates copper tubing along the mold structure, optimized reflective mirrors to concentrate radiation, a transparent glass cover to reduce thermal losses, and an insulated 60L thermal storage tank. Testing was conducted in Basra, Iraq, from January 2017 to May 2019 across diverse climate conditions. At a constant mass flow rate of 170 ml/min, the maximum outlet temperature reached 97°C under 1024 W/m² solar intensity, and up to 70°C during cloudy conditions. The collector achieved an average experimental thermal efficiency of 81.6%, which was validated through theoretical modeling of solar angles, buoyancy-driven flow, and heat transfer. Economic analysis demonstrates that the system can be manufactured cheaply using local materials, making it a viable alternative to conventional flat plate collectors for residential and remote applications in high-irradiation regions.

Keywords: Solar collector, Global warming, Solar heater, Basic structure, Siphon circle, Cake Mold, Efficiency

1. Introduction

The sources of renewable energy are those that generate naturally and constantly as long as the sun exists. Solar energy is considered the most important one for humans and can be exploited. It is a permanent energy that does not result in gases or by-products that harm the environment like other energies and does not cause dangerous remnants like radioactive residue from nuclear power [1], [2], [3].

Now, solar energy has a special position among other sources. Solar thermal energy has increased and become a significant source of renewable energy because of an increase in environmental effects as well as the rising cost of fuel types (i.e., oil or gas, such as global heating, greenhouse effects, air pollution, and the reduction of the ozone layer) [4], [5]. Most countries put big budgets into this energy. There are many ways to use it, like collecting the heat of the sun and absorbing it, as in this research, transferring sunlight to electrical power, or through other means [6], [7].

The usage of solar power for heating water has been known for a long time. Heating systems were developed at the beginning of this century because of the need to use them in remote areas instead of traditional power sources. Iraq has a significant potential for solar energy for both power production and thermal applications from solar energy technologies [8]. The two problems were reflected in the economy and the lives of the people who lived there [9].

The production of hot water in most areas is promising for the application of solar energy. A solar heater is the best application for solar energy because it is easy to manufacture and has low cost [10]. In this research, CM is supplied with an isolated thermal tank (T-Tank) to store hot water. In recent years, the demand for energy has increased, and fears have grown because of two factors: environmental impacts result from the burning of huge amounts of fossil fuel, and the lack of acknowledgment about the increasing need for current global reserves [11]. On the other hand, a big share of productive energy in the world is used to heat water in houses [12]. Energy consumption increasingly depends on population growth and the update of productive processes [13].

The global demand for energy increases with the encouragement of research towards alternative technology [14]. Renewable energy contributes to reducing the consumption of these kinds of fuel. As a result, the above-mentioned problems are reducing [15].

The source of renewable energy plays an important role in the exchange of traditional fuel in four distinct zones, such as the production of electric power and hot water, transportation of fuels, and power services in the countryside [16]. Alternative energy sources, in many countries, are available and are being applied, such as wind, solar energy, photovoltaic energy, and others. Among these applications is solar thermal energy for water heating. Solar energy is important because it is economical, environmentally friendly, and widely available [17], [18].

The use of solar technology has increased since 1980 by 30% annually [19], [20]. In 2010, the Renewed Energy Policy Network stated that 70 million houses in the world are using hot water systems with solar energy (SWH) [21]. The number of applications for hot water in houses has increased by 85% [22]. Solar energy, which can be successfully used to provide technological and household needs, and for heating in various industrial processes, and the general sector [23][24].

Solar heaters or collectors are systems that apply solar energy to heat water [25]. The use of solar heaters and collectors in different applications requires solar energy and the development of their types, like flat plate collectors (FPC), hybrid photovoltaic/thermal collectors (PV/T), compound of vacuum tubes, compound of parabolic collectors, etc. Solar concentrating collectors direct solar radiation from a larger field to a small receiving area where it is converted into other forms of energy [26], [27].

Recent research trends have focused on improving collector performance through several strategies, including geometric optimization, incorporation of reflective surfaces, enhancement of heat transfer mechanisms, and reduction of thermal and radiative losses [28], [29], [30]. Various studies have shown that modifications in collector geometry and the use of reflective mirrors and booster reflectors can significantly increase the effective solar absorption area without substantially enlarging the collector footprint. Similarly, enhancements such as turbulence promoters, surface texturing, and advanced absorber coating have been investigated to increase convective heat transfer and reduce thermal resistance [31], [32].

However, many of these advanced configurations rely on complex manufacturing processes, specialized materials, or high-cost components, which restrict their practical implementation, especially in developing countries and remote regions with limited technical infrastructure and economic resources. As such, there remains a critical need for innovative solar collector designs that not only achieve higher thermal performance but also maintain structural simplicity, low production cost, and ease of local fabrication [33], [34].

In this context, the current study introduces a new solar heater design based on a cake mold (CM) geometry that aims to overcome the limitations of conventional systems by enhancing absorption efficiency, improving operational stability under variable weather conditions, and offering a cost-effective solution for decentralized water heating applications.

2. Materials of solar heaters (CM)

The basic structure of the construction of CM is an iron plate with a thickness of 0.1 cm, a square iron pipe with ribs of 2.5 cm, a copper pipe with a diameter of 0.956 cm and a length of 2540 cm for circulation, locally available reflective mirrors of various sizes, and a 5 cm aluminum holder. Sealing is done using silicone, and the coverage is provided by a transparent glass sheet of 110×110 cm² thickness of 0.4cm. A plastic pipe is used to link CM with the external water tank (EWT), and matte black paint is used to increase heat absorption. Lastly, an isolated thermal tank (T-Tank) with a tank size of 60 L, which is enough to store heated water, is used for efficient performance and usability.

3. Experimental setup

The structure of CM is like a cake mold. The design gives the path of the cooling for the copper pipe installed inside it with less space, which gives enough time for the water to acquire more heat in less time (speed of heating). Moreover, the design is modern and highly efficient, needs no big space, produces more than 100 L/m², is easy to clean, move, and maintain, works in different weather conditions like cloudy weather, and has a long running age (Figure 1).

Figure 1. The basic structure of CM

The basic structure of CM consists of:

a. The front face is circular in diameter of 110 cm.

b. The base of the structure is circular in diameter of 70 cm.

c. The distance between the front face and the base is 50 cm.

d. The heart of the structure is cone-shaped, which is 43 cm high, 29 cm in diameter at the base, and 3 cm in diameter at the top.

e. The foundation, which supports the basic structure, is square in shape. The length of the rib is 150 cm, which consists of a square iron pipe, the length of which is 2.5 cm.

That is, the area of the front facade of the solar collector CM is 9498.5 cm² (Figures 2 and 3).

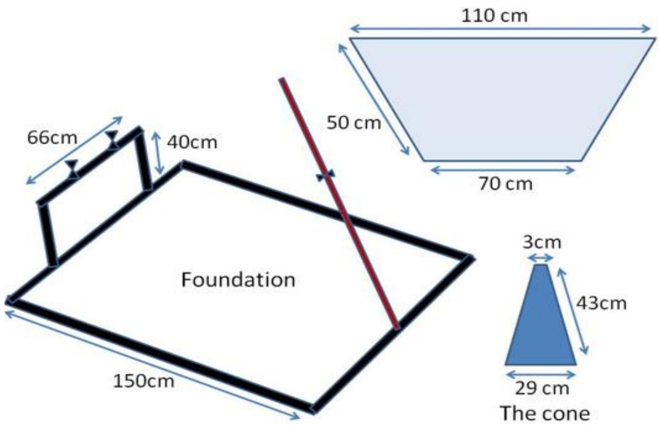

Figure 2. The details of the basic structure of CM

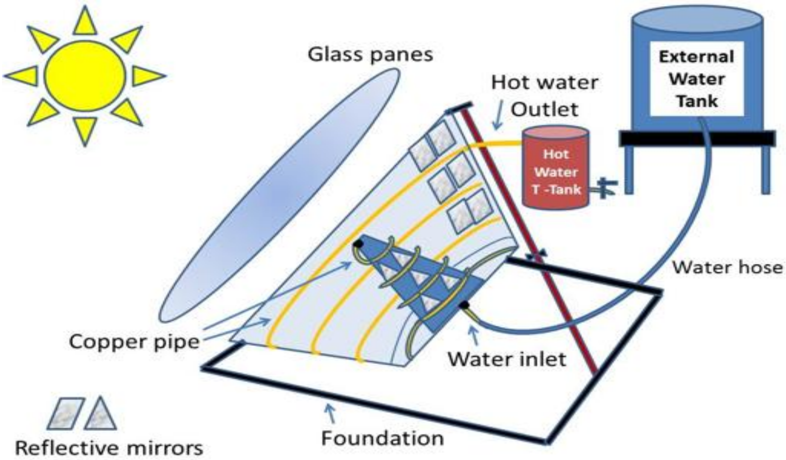

Figure 3. The diagram of CM

The aluminum holders are fixed on the inner surface at equal distances to raise the copper pipe by a distance of 5 cm on the inner surface of the structure, as in Figure 4:

a. The holders are fixed on the inner surface between the front face and the base.
b. The holders are fixed on the base's structure from inside.
c. The holders are fixed on the outside surface of the cone.
d. The holders are fixed on the outside surface of the cone.

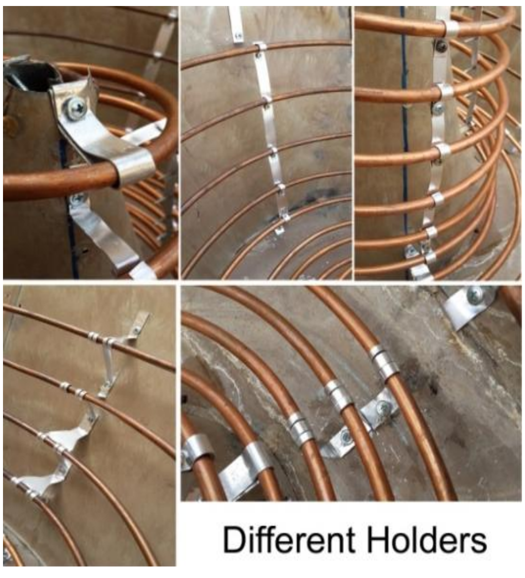

Figure 4. The types and positions of aluminium holders in the CM

Heating and cooling applications and water heating are considered low-temperature applications. But the high temperature is generated by the concentration of solar radiation by the reflective mirrors, at one point or line. The CM's direction must be toward the sun, so the solar radiation is vertical on the heater's surface to ensure the concentration of solar radiation and to get high efficiency. In CM, all falling solar radiation reflects on the copper pipe installed in it to cause the rising of temperature. The use of flat mirrors causes the dispersion of some reflected rays and does not fall on the passing pipe, so small pieces of mirrors are used to reduce the dispersion and to increase concentration. The cake mold shape is useful for dispersing rays. Reflected solar radiation is the main radiation for another mirror; this means that the radiation is reflected again to another pipeline, as in Figure 5.

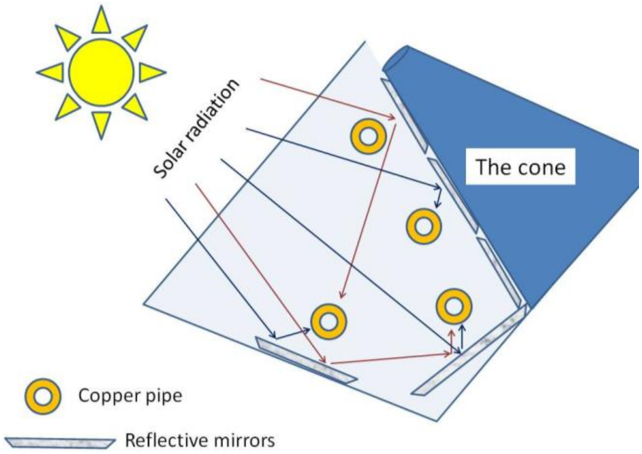

Figure 5. The reflected solar radiation from mirrors

The reflective mirrors are fixed with silicone inside the CM after the installation of pipe holders. These mirrors help in raising the water temperature that passes through the copper pipe by reflecting solar radiation towards it.

Different-sized mirrors are used because of the shape of the structure, as follows:

a. Reflective mirrors in the size of 8 x 8 cm^2 are installed on the inner wall of the structure.

b. Reflexive mirrors in different sizes 8–16 cm^2 are installed on the outer wall of the cone. These mirrors take the shape of a cone.

c. Reflexive mirrors, size 12 x 10 cm^2, are installed on the base of the structure, tilted at a small angle towards the cone as illustrated in Figures 5 & 6.

Figure 6. The installation of reflective mirrors and copper pipes with matte black paint

Copper has the ability to form high connections and is easy to roll, so it can transfer high temperatures even when the temperature differences are low. A copper pipe with a diameter of 0.956 cm and a length of 2520 cm is installed on aluminum holders in the solar heater. The distance between the copper pipe and reflective mirrors is 5 cm. The rolling of the copper pipe starts from the top to the base of the structure, after that continues towards the base of the cone till it reaches the top, and then it gets out from the center of the structure to the back side of the basic structure. The copper pipe is painted matte black to absorb more heat, as in Figures 1 and 6.

The capacity of the copper pipe is 6.8 L. The first end of the copper pipe in the center of the solar heater connects with an external tank by a plastic pipe, which supplies CM with water. The other end of the copper pipe passes through the wall of CM from the top as a way to get out the hot water (Figure 7).

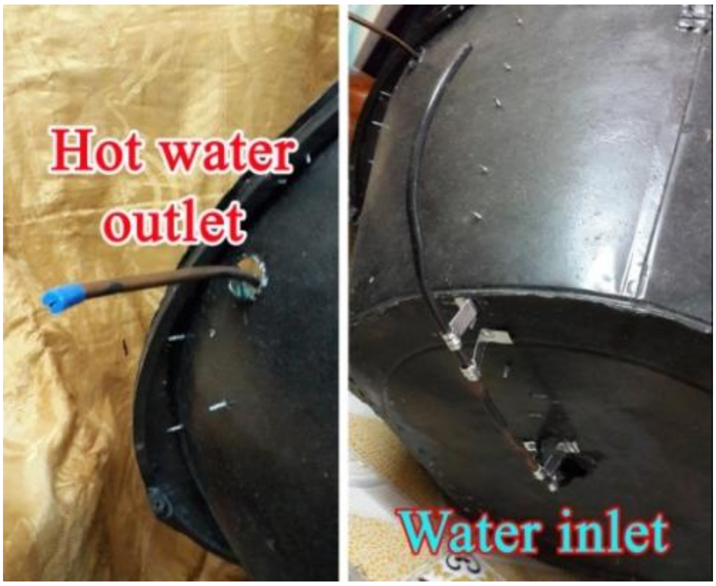

Figure 7. Water inlet and hot water outlet to CM

A transparent glass sheet, cover in thickness of 0.4 cm and a size of 110 x 110 cm^2 put on the front face of the solar heater because of:

a. The ease of cleaning the face of CM.

b. The rising temperature inside CM because of global warming.

c. Reducing the thermal damage from the load and radiation. The glass prevents the exit of reflected radiation from the pipe and the mirror, in addition to the thermal damage from the load. The glass allows 90% of short-wave solar radiation to enter the copper pipe and mirrors, whereas it prevents the exit of long-wave radiation reflected from the copper pipe (Responsible for the water heating) from the copper pipe.

A T-tank was added to improve the work of CM, with a capacity of 60 L. It collects the output hot water from CM to use in houses, schools, pools, remote places that have problems with electrical energy, moving labs near the wells, etc.

The CM must be directed towards the sun to have more solar radiation. The degree to which CM leans on the horizon depends on the latitude of the area and the time during the year. Basrah city is at a longitude of 47°45' and a latitude of 30°33 ', so the tilt angle of the solar heater in summer is 15° and in winter 45° [35]. The process of controlling the direction of the CMs collector so that it is always perpendicular to the solar radiation for getting high efficiency was in a manual fashion.

CM tested:

1. From January 2017 to May 2018
2. From January 2018 to May 2019

There was no difference in the work of CM during the two periods, and it shows stability. After exposure of CM to the sun, be orthogonal to solar radiation during daytime, it starts to acquire heat by (direct solar radiation, reflection of radiation by the reflective mirrors, global warming in the CM room). The water that passes through the copper pipe heats till it reaches more than +97C° from during the control of water flow, 170 ml/min, in the pipe and the transmission of the temperature by connection, load, and radiation. The output hot water collects in the T-Tank. 5L draws from the T-Tank during the test each hour to use, and to register the temperature of output water from CM, and the temperature of the T-Tank water is 70C°.

CM was also tested in:

1. Cloudy weather
2. Stormy, partly cloudy weather. The design of CM works efficiently during the test. It registers 48-70C° in cloudy weather, and the temperature of the T-Tank is 63C°.

4. Theoretical analysis for CM

Anywhere, economic evaluation and detailed information on the availability of solar radiation are important to solar energy systems. The solar radiation that falls on a surface consists of:

- The location of the sun
- Surface direction

Figure 8 shows the solar angles for the solar collector with the sun, given that the collector is a sloping surface.

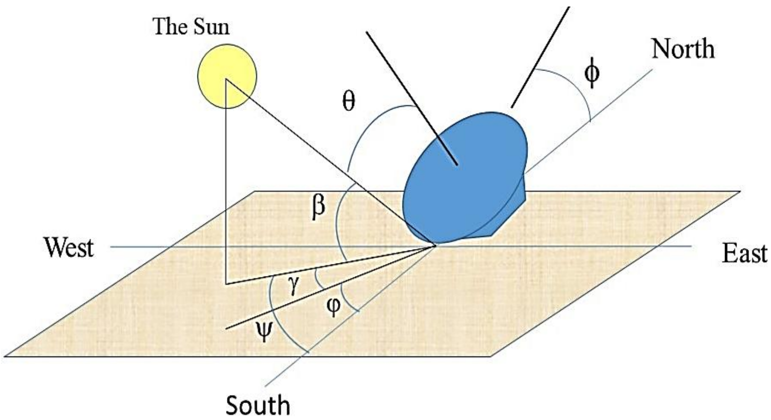

Figure 8. The solar angles for the surface of the inclined collector.

• The sun's place is a function of the latitude (L), the time (t), the solar year day number with 1st January (D), and the solar inclination (δ). This information is given in the following equations because of the basics of physics and solar engineering [36].

$$\delta = 23.5\ \sin\left[(D-80)\frac{360}{365}\right] \tag{1}$$

$$\tau = 15(t-2) \tag{2}$$

$$\sin\beta = \sin L \sin\delta + \cos L \cos\delta \cos\tau \tag{3}$$

The angle θ of solar rays on a surface tiled with the level by the angle ϕ is given by the relation [36], [37]:

$$\cos\theta = \cos\beta \cos\gamma \cos\phi + \sin\beta \cos\phi \tag{4}$$

The following relation gives the angle of the solar azimuth [38] :

$$\sin\Psi = \cos\delta \sin\tau / \cos\beta \tag{5}$$

φ = 0 when the CM is towards the south, so that $\gamma = \Psi$ and then:

The following relation gives the intensity of solar energy on the surface of the collector [39]:

$$I = ae^{-b/\sin\beta}\cos\theta \qquad (6)$$

a and b are monthly subordinate parameters tabulated.

The rate of water mass flow through the CM can be evaluated from thermal balance and mass transfer balance between the buoyancy and compression in the siphon circle due to:

- The difference in density of cold and hot water.
- The compression losses in the collector tubes, as in Equation 7:

$$\Delta P_B = \Delta P_f \qquad (7)$$

ΔP_B is the driving force of the natural cycle.

ΔP_f is the total pressure drop along the circle (Figure 9).

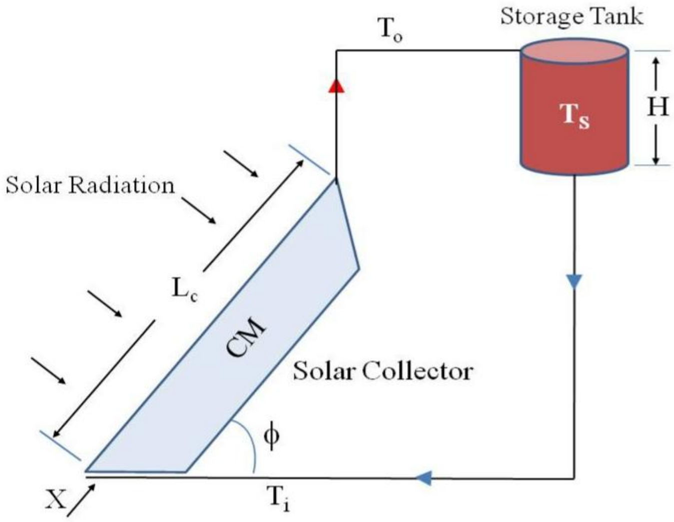

Figure 9. Solar water heater system CM with the siphon circle

ΔP_B consists of:

a. ΔP_C: the compression drop through the collector.

b. ΔP_S: the compression drop between the top and bottom of T_S.

Where T_S is the water storage tank.

$$\Delta P_B = \Delta P_C + \Delta P_S \qquad (8)$$

The following equation represents the compression caused by the buoyancy force ΔP_B [40]:

$$\Delta P_B = g\beta'\rho_o \sin\phi \int_0^{Lc} (T(X) - T_i)\, dx + g\beta'\rho_o (T_o - T_i)\, H \qquad (9)$$

The following linear equation represents the temperature distribution in the tubes:

$$T_{(X)} - T_i = \frac{To - Ti}{Lc} X \qquad (10)$$

Integrating equation (9):

$$g\beta'\rho_o (T_o - T_i)\left[\frac{Lc \sin\phi}{2} + H\right] \qquad (11)$$

Frictional resistance is equal to the buoyant force in the water flux path at the equilibrium. This means:

$$\Delta P_f = \Delta P_B = g\beta' \rho_o (T_o - T_i) \left[\frac{Lc \sin\phi}{2} + H\right] \quad (12)$$

The following equation represents the friction drop in the tubes:

$$\Delta P_f = \frac{1}{2}\rho f \frac{u^2 Lc}{2\, dc} \quad (13)$$

To arrive at a laminar flux, f is given by the following equation:

$$f = \frac{64}{Re} = \frac{64\nu}{dc\, u} \quad (14)$$

The mass flux rate ($\dot{m}$) depends on the number of parallel tubes (N) in the solar collector, as follows:

$$\dot{m} = \frac{\pi}{4} N \rho u d_c^2 \quad (15)$$

OR

$$u = \frac{4\dot{m}}{N\rho\pi dc^2} \quad (16)$$

From equation 12 to equation 16, the following equation appears:

$$128 \frac{\nu\, Lc\, \dot{m}}{\pi\, N\, dc^4} = g\beta' \rho_o \ (T_o - T_i) \left[\frac{Lc \sin\phi}{2} + H\right] \quad (17)$$

(T_o - T_i) can be written from the heat balance of the solar collector in the equation:

$$(T_o - T_i) = \frac{I\,\alpha\, Ac - h\, Ac\, (Tm - T\infty)}{\dot{m}\, Cp} \quad (18)$$

Where

$$T_m = \frac{(T_o - T_i)}{2} \quad (19)$$

The heat transfer coefficient can be given as a function of wind speed in the following equation [41]:

$$H = 2.8 + 3u_{wind} \quad (20)$$

5. Storage tank in solar system

To find out the energy balance, a thermally insulated storage tank can be looked at, as follows:

$$Mc_p \frac{dTs}{dt} = \dot{m} c_p (T_o - T_i) \quad (21)$$

($\dot{m}$) and (T_o - T_i) varies with time, as the solar incidence varies through the daylight.

6. Solar density

In Basrah city, the solar incidence on the surface depends on many variables:

a. Solar inclination (δ).

b. Time (t).

c. Latitude (L).

d. Surface azimuth angle (φ).

e. Surface-solar azimuth angle (γ).

f. Surface angle with the level (ϕ).

From knowing the variants and using equations 1 to 6, solar incidence can be calculated.

Basrah city is located at a latitude of 30° 33' in southern Iraq [42]. With a south-facing surface from 8:00 am to 5:00 pm on 20-Jan 2019, the data from equation (6) is processed as follows:

$$I=(114\phi^3-753\phi^2+1030\phi+640)\sin\left[\frac{\pi t(\text{in hours from the sunrise})}{\text{daylight(in hours)}}\right] \quad (22)$$

For the last years from 2009 to 2019, the weather in Basrah city on 20-Jan is:

- The maximum temperature is (8-16) °C.
- The wind speed is (2-8) m/s.

In Table 1, the engineering information for the solar collector CM is included, giving physical properties of water used through specific relations [43]:

Table 1. The physical and engineering information of the CM

Physical and engineering data for CM	The value
CM area A	9498.5 cm^2
Number of CM tubes in parallel N	17
Total diameters pipe parallel in CM is d_c	N x 0.956 = 16.525 cm
Volume of water storage	60 lit
Absorptivity α_{cp}	0.97
r	$1001-0.08832T-0.003417T^2$
c_p	$4226-3.244T+0.0575T^2-0.0002656T^3$
β'	$(0.3+0.116T-0.0004T^2)10^{-4}$
υ	$((1/0.5155+0.0192T)-0.12)10^{-6}$

The expense of thermal efficiency to the solar collector using equations [44]:

$$Q = I\,A_{cp}\,F_t\,(\tau_g\,.\,\alpha_{cp}) \quad (23)$$

Where:

Q : The amount of energy absorbed

I: Total solar radiation falling on the surface of the solar collector (W/m^2)

A_{cp}: The surface area of the copper pipe(m^2)

F_t: Coefficient of the effect of shadow and dust on the amount of solar radiation received

α_{cp}: Absorbitivity the copper pipe

τ_g: Permeability of the glass cover

$\alpha_{cp} = 0.97$, $\tau_g = 0.95$ [45]

$$F_t = F_d.\,F_{sh} \quad (24)$$

Where:

F_d Coefficient of the effect of atom dust on the glass cover on the solar radiation recipient.

F_t Coefficient entering the effect of shadow covering the part from the absorption tube on the solar radiation recipient.

$F_d = 0.97$, $F_{sh} = 0.98$ [46]

$$Q_u = M\, C_w\, (T_{av} - T_i) / t \qquad (25)$$

Where:

Q_u: The useful energy

M: Mass flow rate (kg s)

C_w: Specific thermal capacity (J/ (kg· C)

T_{av}: Rate water temperature outside the collector (C°)

T_i: Inlet water temperature (C°)

t: Operating time sec (s)

The average efficiency was produced based on the equation [47]:

$$\eta = (Q_u / A_{CM} \,.\, I_{CM}) \times 100 \qquad (26)$$

Where:

Q_u: The useful energy.

A_{CM}: The collector area (m²)

I_{CM}: Solar radiation (W/m²)

The solar radiation exposed the solar collector CM with a density (834-1024) W/m², and solar radiation was detected by a pyranometer in Basrah city, as shown in Table 2. Using equations 23, 24, 25, and 26, the thermal efficiency of the solar collector is 81.6 %.

Table 2. The data for calculating the thermal efficiency to CM

Time	The data	Dec-18	Jan-19	Feb-19	Mar-19	Apr-19	May-19
01:00	Tav (C°)	91	87	91.5	95	96.5	97
	Ti (C°)	23	19	25	27	31	34
	M (Kg)	10.5	10.5	10.5	10.5	10.5	10.5
	C_w (J/Kg.C°)	1	1	1	1	1	1
	t (hr)	1	1	1	1	1	1
	Qu (W)	714	714	698.3	714	687.8	661.5
	I_{CM} (W/m²)	834	830	848	944	964	1024
	A_{CM} (m²)	0.95	0.95	0.95	0.95	0.95	0.95
	η (%)	77	79.6	79.7	79.6	75	68
	$(T_{in} - T_a) / I_c$ (C°.m²/W)	0.047	0.041	0.039	0.038	0.032	0.030

7. Results and discussion

CM tested and registered the temperature during exposure to the solar radiation from:

a) December 2017 to May 2018 from 8:00 am to 5:00 pm.

b) December 2018 to May 2019 from 8:00 am to 5:00 pm.

Diagrams 10 and 11 show the behavior of CM while working and the large increase.

In the temperature of the output water from CM, the water acquires a high temperature during the pass through the heater. The large increase in temperature happens because of the shape of CM, the fall of direct radiation, global warming, the distribution of reflective mirrors for the reflection and concentration of solar radiation on the copper pipe, and the direction of CM being orthogonal to solar radiation.

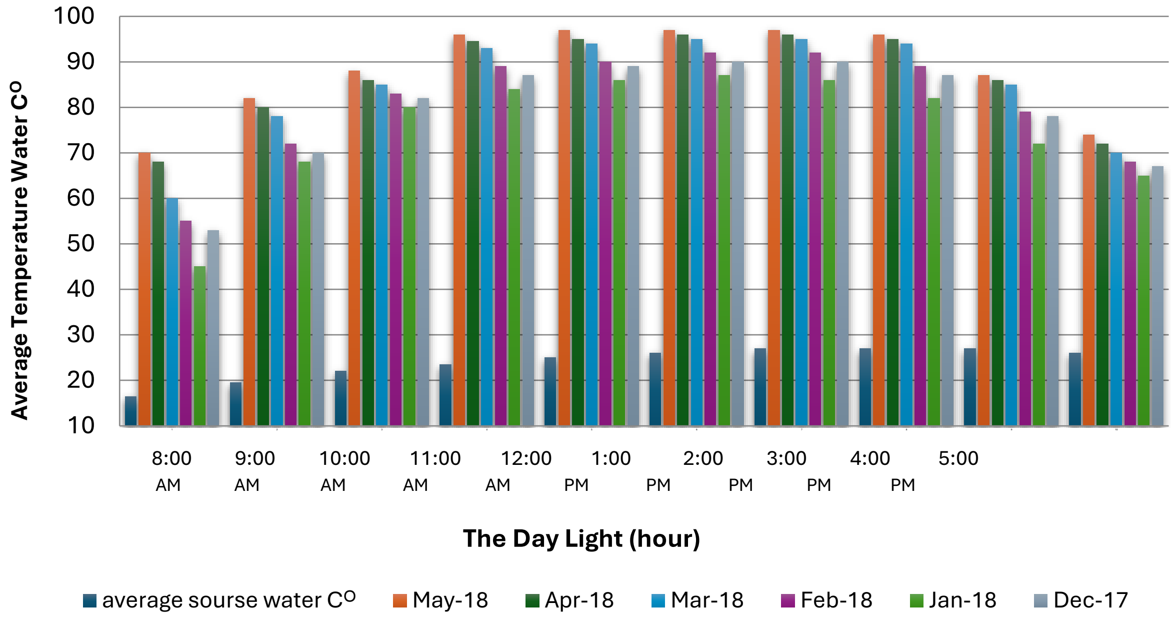

Figure 10. Average water temperature from CM per month from Dec 2017 to May 2018.

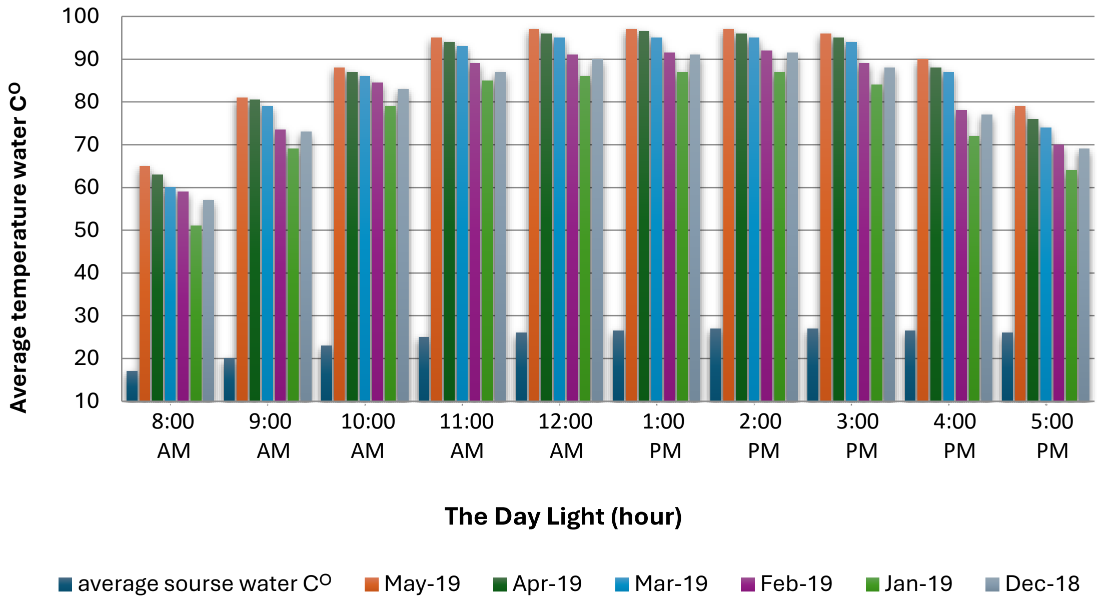

Figure 11. Average water temperature from CM per month from Dec 2018 to May 2019

Diagrams 10 and 11 show the stability of CM's work. The running age of CM's design in different circumstances is from 3 to 5 years, because of the length of the testing period and the stability of CM's work.

Tables 3 and 4 show the monthly average of the lowest and highest temperatures of output water from CM when the water flow is 170 ml/min during December 2017 to May 2018 and December 2018 to May 2019, during the daytime from 8:00 am to 5:00 pm.

Table 3. The monthly average of the lowest and highest temperatures of the output water from CM during 2017- 2018

Average monthly (Lowest - Highest) temperature C^O from CM through the daytime hours in 2017-2018											
Dec-17		Jan-18		Feb-18		Mar-18		Apr-18		May-18	
Less	Highest	Less	Highest	Less	Highest	Less	Highest	Less	Highest	Less	Highest
53	90	45	87	55	92	60	95	66	96	68	97

Table 4. The monthly average of the lowest and highest temperatures of output water from CM during 2018-2019

Average monthly (Lowest - Highest) temperature C^O from CM through the daytime hours in 2018-2019											
Dec-18		Jan-19		Feb-19		Mar-19		Apr-19		May-19	
Less	Highest	Less	Highest	Less	Highest	Less	Highest	Less	Highest	Less	Highest
57	91.5	51	87	59	92	60	95	63	96	65	97

The temperature of output water from CM is more than +97C° and the temperature of collected water in the T-Tank is 85C°, specified for different uses; these temperatures are very high compared with flat plate heaters. Figure 12 shows the monthly average of the temperature of collected water in the T-Tank specified for different uses in houses, institutions, mobile laboratories, and pools. This gave 122.4 L/day with a collector area of 0.95 m².

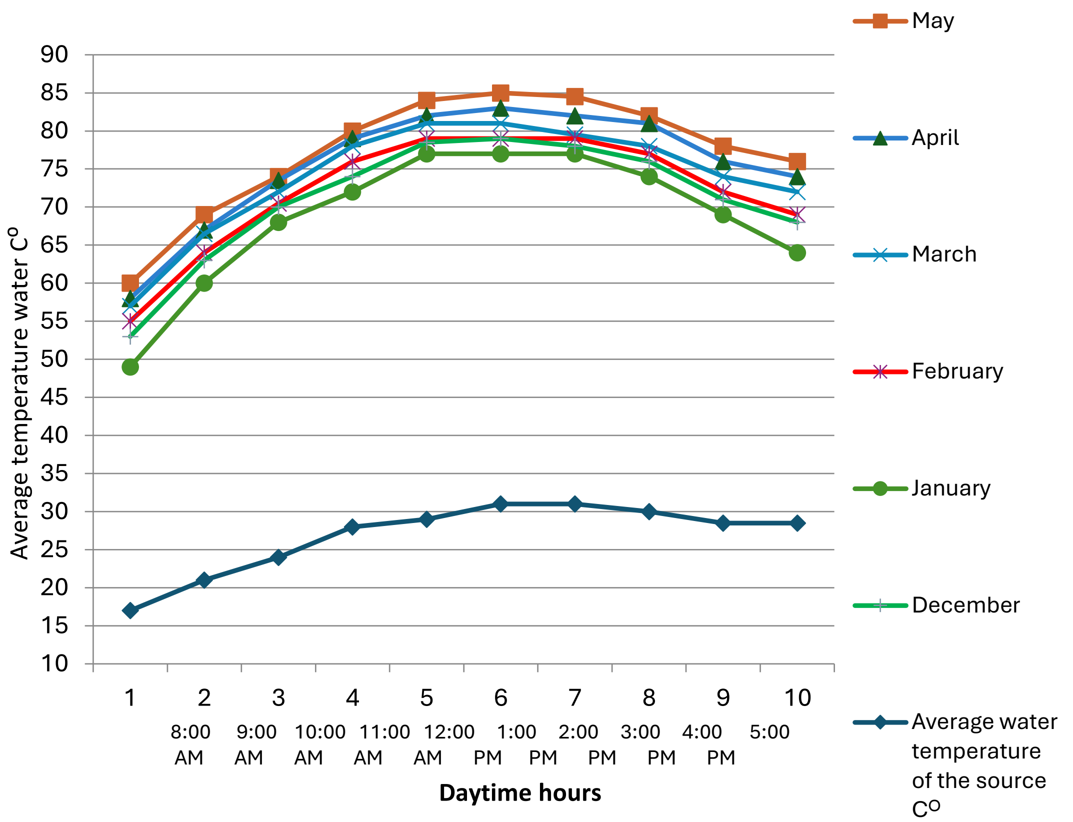

Figure 12. The monthly average water temperature collected in the T-Tank

CM was tested in cloudy weather on 5-May-2018 at a temperature of 37 C° during daytime from 8:00 am to 5:00 pm. CM was tested in stormy, partly cloudy weather on 16 February 2019 at a temperature of 21C° during daytime from 8:00 am to 5:00 pm. The results are shown in Table 5 and Figures 13 & 14.

Table 5. CM in stormy, partly cloudy, and cloudy weather through the day

Cloudy weather			Stormy, partly cloudy weather		
(5-5-2018) -37 C^{O}			(16-2-2019) - 21 C^{O}		
Time	Tow C^{O}	T-Tank C^{O}	Time	Tow C^{O}	T-Tank C^{O}
08:00	48	44	08:00	42	38
09:00	62	57	09:00	51	47
10:00	67	58	10:00	60	52
11:00	68	60	11:00	66	59
12:00	69	63	12:00	69	62
01:00	70	63	01:00	70	63
02:00	70	63	02:00	70	63
03:00	69	63	03:00	68	63
04:00	66	63	04:00	63	62
05:00	60	61	05:00	58	60

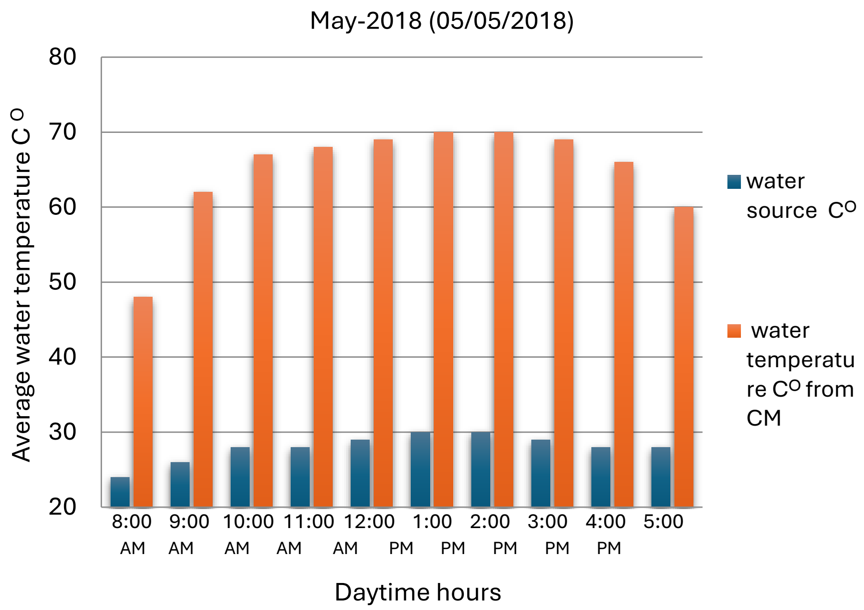

Figure 13. The average water temperature CM in cloudy weather on 5/5/2018

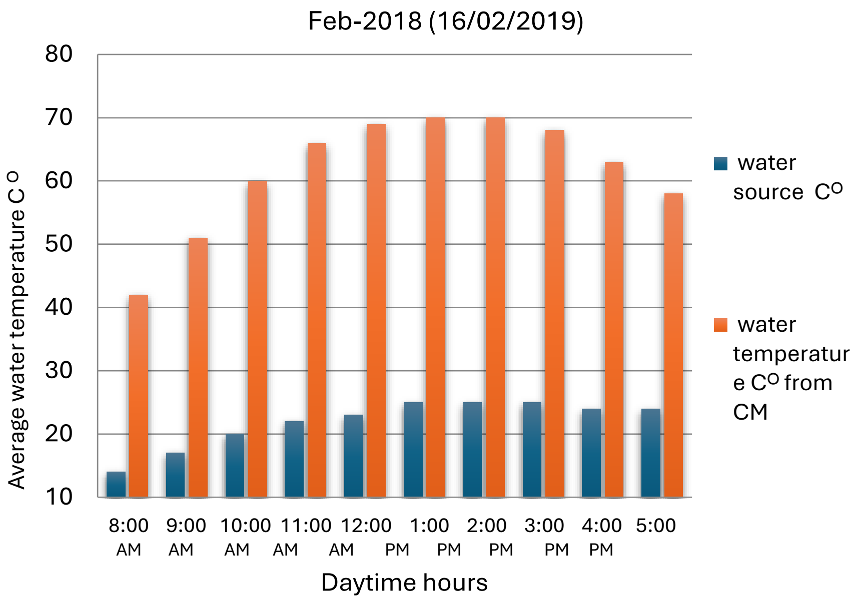

Figure 14. The average water temperature CM in stormy partly cloudy weather on 16/2/2019

In this research and Figure 1, angles β and θ are affected by solar radiation incident on the solar collector CM for being italic (Equation 6). These angles can be found from Equations 3 and 4, respectively. When θ = zero, so that $\phi = 45^o$, then the sun's rays are perpendicular to the surface of the solar collector.

Observed in Figure 15 on 20-Jan, the altitude angle β increases from zero with the beginning of the daylight, even up to the peak at midday, but this angle decreases even up to zero, but this angle decreases even up to zero by the end of the daylight, and the highest value of altitude angle β at latitude 30° 33' is 45^o, and inclination angle is -20^o.

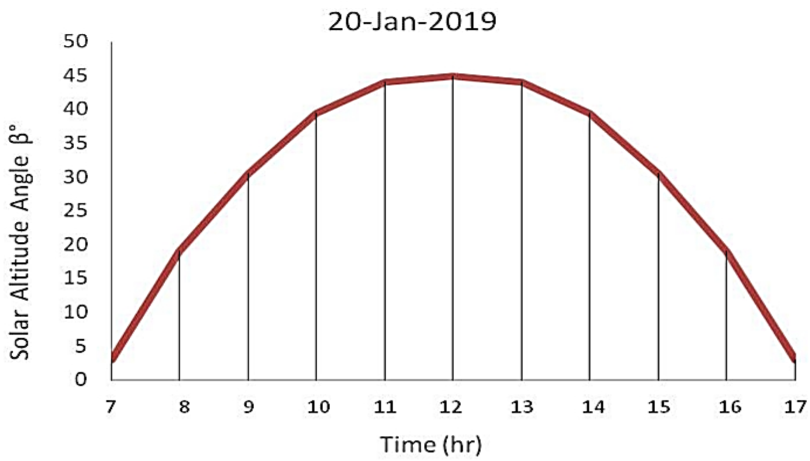

Figure 15. Solar altitude angle during daylight hours in Basrah City on 20-Jan-2019

In Figures 8 & 16, as the level angle ϕ increases, the solar incident on the inclined collector surface reaches the peak value at $\phi = 45^o$, and it decreases after that. This means that the maximum solar radiation can be obtained when the CM faces direct vertical radiation.

At midday, the angle γ = zero, and from Equation 4: $\theta = 90 - \beta - \phi$. Where $\beta = 45^o$ when the collector surface is facing south, and the angle $\theta = 45 - \phi$, which θ = zero when $\phi = 45°$, then the sun's rays are perpendicular to the solar collector surface CM, which is the maximum solar radiation incident (normal) on the inclined collector surface.

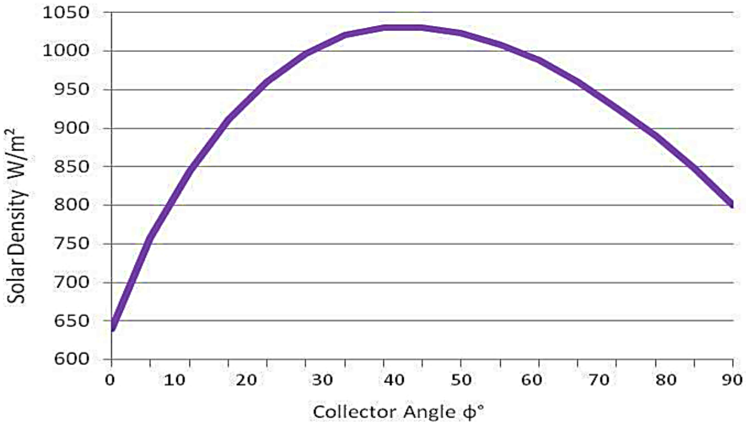

Figure 16. Shows solar density with the angle of collector tilt ϕ

By using equations 17 and 18 with Euler's method, Equation 21 is a numerical solution to calculate Ts, as shown in Figures 17-22. Figure 17 shows the effect of ϕ on the stored water temperature. Ts increases with increasing ϕ for the loop considered; solar radiation increases.

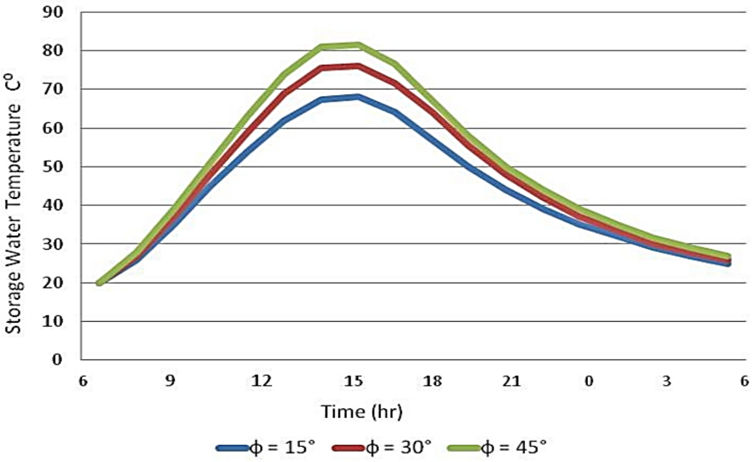

Figure 17. The effect of (ϕ) with the Level on the stored water temperature

Choosing the design of the collector in the form of a cake mold, gives more exposure area to the solar radiation as in Figure 18, reducing heat loss due to the wind, as in Figure 19, and it compensates for the low water temperature due to the large volume of stored water in the T-Tank, where the heat is absorbed by the water (Figures 18 and 20).

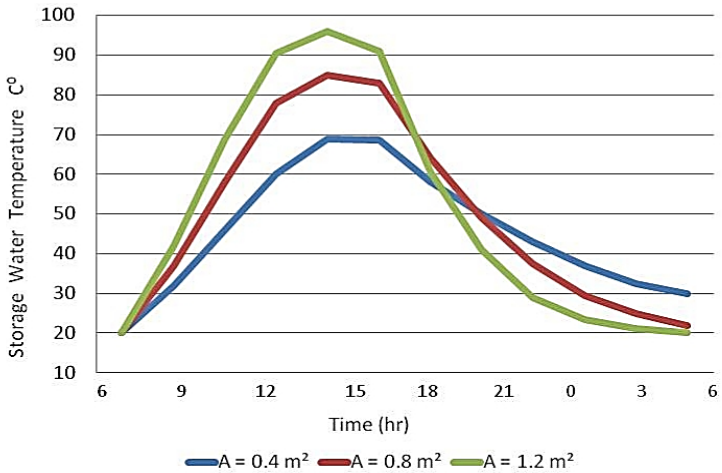

Figure 18. Variation of the stored water temperature with the collector area

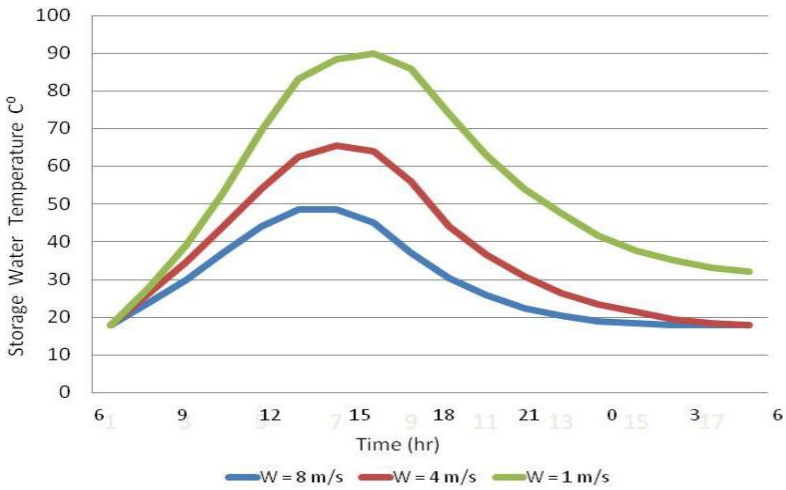

Figure 19. Variation of the stored water temperature with wind speed

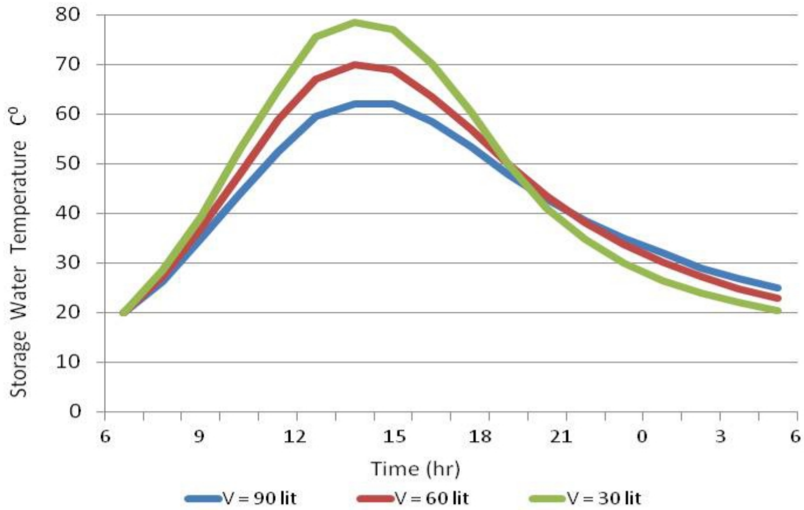

Figure 20. Variation of the stored water temperature with the storage water volume

The maximum solar density is at midday; the density increases with the angle ϕ from 15º to 50º of the collector, and the solar radiation is perpendicular to the collector surface when ϕ = 45º, as shown in Figures 16 and 21.

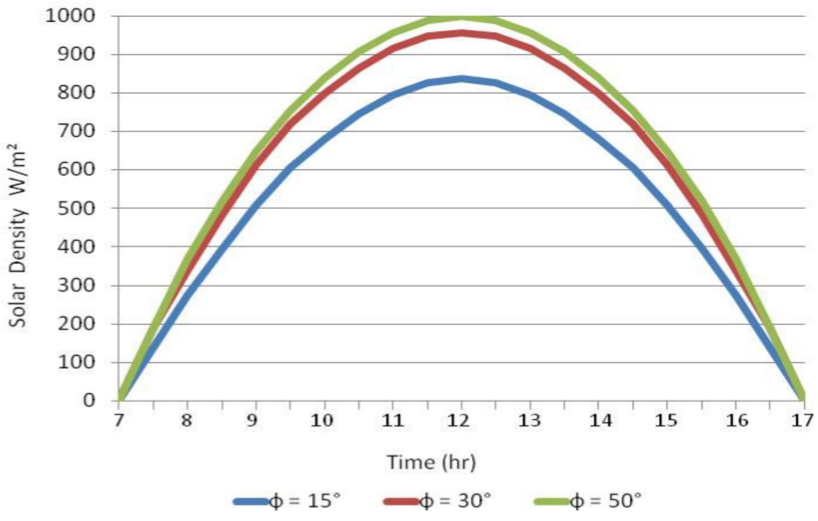

Figure 21. Variation of the solar density with the tilt angle ϕ

Figure 22 shows the water outlet at the CM exit, and T_o increases with ϕ, when ϕ = 45º, reaching a peak value.

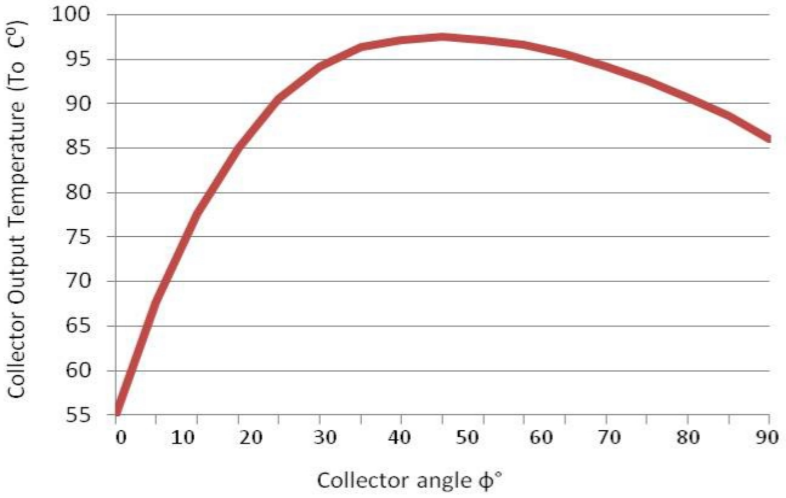

Figure 22. The output water temperature with the angle of collector tilt ϕ

From Figure 23 and Table 2, the thermal efficiency of the solar collector in the winter is above the thermal efficiency in the summer due to the difference in water temperature entering the collector and solar radiation.

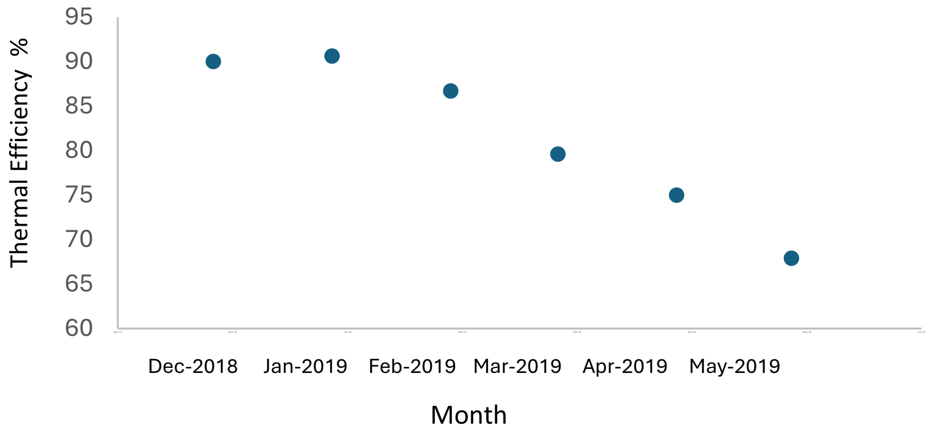

Figure 23. The monthly thermal efficiency of the solar collector CM

The calculated thermal efficiency (η %) is obtained by graphing $(T_{in}-T_a)/I_{cM}$ versus collector thermal efficiency (η_{CM} %), as shown in Figure 24. From the analysis of the graph, it is observed that the curve represents heat loss from the solar collector CM.

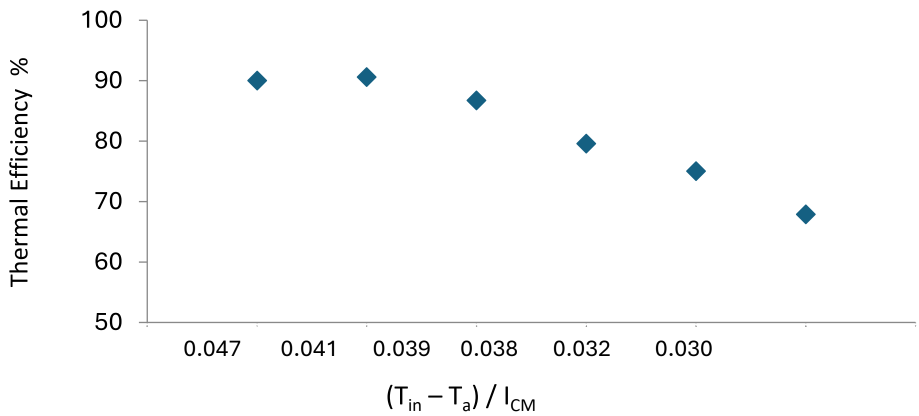

Figure 24. Thermal efficiency of solar collector CM with $(T_{in}-T_a)/I_{CM}$

Raw materials available on the local market were used, according to the current price of the materials (1 U.S. $ = 1320 I.D.). The cost of manufacturing the solar heater CM is shown in Table 6.

Table 6. The cost of manufacturing the CM design

Materials	The number	The cost I.D CM
Transparent glass sheet, thickness is 0.4 cm	110 x 110cm²	3000
Iron plate, thickness is 0.1 cm	100 x300 cm²	9000
A plastic pipe	300 cm	750
Copper pipe, diameter is 0.95 cm	2540 cm	25738.5
Mirror thickness is 0.3 cm	100 x300 cm²	7500
The square iron pipe	750 cm	5000
Matte black paint	1	500
Silicone	3	2250
Valve	1	250
Holder of aluminium	-	500
Insulated thermal tank (T-Tank)	1	3000
Total		46000

From Table 6, it was found that the cost of manufacturing the collector CM is suitable for the amount of hot water production, as shown in Tables 3 and 4. If they are produced in a factory and workshops, the cost is much lower because the raw materials are at wholesale prices. The study can be developed more and more by wireless techniques and the Internet of Things [48, 49] as well as antenna sensors [50].

8. Conclusion

CM is a new design that can be fabricated in small and large workshops, which provides ease of cleaning, maintenance, and transport. The manufacturing price is low and can be lower by using aluminium pipes rather than copper, while all the materials needed are easily available in the local market. It provides an output water temperature of more than 97 °C and keeps the circulating water in the T-Tank at 85 °C, with a stable collector flow rate of 170 ml/min, which corresponds to a collector area of 0.95 m² and an output of 122.4 L/day. Even in bad weather or cloudy conditions, with a temperature of 70 °C in the output water and 63 °C in the T-Tank, CM can be operated efficiently, with an average thermal efficiency of 81.6%. Frequently tested and known to have a long service life of 3-5 years, it will perform well in all weather conditions. The optimum tilt angle is 45° - 50° S in Basrah City, but the performance is highly dependent on the location, collector orientation, tilt, wind speed, and daylight duration. It did not, however, go into more advanced experimental durability, corrosion, or climate testing and expects more tests to be carried out on the real system to prove reliability and environmental durability before widespread application.

Acknowledgements

The researcher would like to thank the Department of Physics, College of Education for Pure Science, University of Basra, for providing facilities to complete the research. This work was partially supported by Southern Technical University under scientific research awards, No. 9/7934, 10 Sep. 2025.

Declaration of competing interest

The authors declare that they have no known financial or non-financial competing interests in any material discussed in this paper.

Author contribution

Rusul Dawood Salim, Wasan L. AL-SALIM: Conceptualization, methodology design, architectural analysis, data collection, and drafting of the manuscript. Mazin Jawad Kadhim, Jassim M. AL-ASADI: Theoretical framework development, heritage identity analysis, data interpretation, and critical revision of the manuscript. All authors contributed equally to the discussion of results, refinement of arguments, and final approval of the version to be published.

References

[1] S. Kuşkaya, F. Bilgili, E. Muğaloğlu, K. Khan, M. E. Hoque, and N. Toguç, "The role of solar energy usage in environmental sustainability: Fresh evidence through time-frequency analyses," *Renew. Energy*, vol. 206, pp. 858–871, 2023.

[2] M. Raoof and M. R. Rahimpour, "Fourth generation of renewable energy materials," 2024.

[3] A. O. M. Maka and J. M. Alabid, "Solar energy technology and its roles in sustainable development," *Clean Energy*, vol. 6, no. 3, pp. 476–483, 2022.

[4] I. E. Maree and A. G. Ismaeel, "Experimental and theoretical calculation of efficiency for flat plate solar collectors in Erbil City," *Periodicals of Engineering and Natural Sciences (PEN)*, vol. 7, no. 2, pp. 786–793, 2019.

[5] Wasan L. AL-SALIM and Jassim M. AL-ASADI, "THE EFFECT OF REFLECTOR SHAPE ON THE PERFORMANCE OF SOLAR COLLECTORS," *MINAR International Journal of Applied Sciences and Technology*, vol. 07, no. 03, Sep. 2025, https://doi.org/10.47832/2717-8234.24.17.

[6] P. Jha, B. Das, R. Gupta, J. D. Mondol, and M. A. Ehyaei, "Review of recent research on photovoltaic thermal solar collectors," *Solar Energy*, vol. 257, pp. 164–195, 2023.

[7] S. Hosouli *et al.*, "Photovoltaic-Thermal (PVT) Solar Collector and System Overview," *Energies (Basel).*, vol. 18, no. 21, 2025.

[8] A. A. Khadom, H. B. Mahood, A. A. Mahmmod, Q. Hassan, and H. A. Kazem, "Improving solar water heating performance and reducing emissions by evacuated tube collectors with preheating units: Iraq as a case study," *Appl. Therm. Eng.*, vol. 265, p. 125596, 2025, doi: https://doi.org/10.1016/j.applthermaleng.2025.125596.

[9] F. Wang, T. Rani, and M. A. Amjad, "The asymmetric impact of energy shortages on sustainable development, human development and economic growth in South Asian countries: The moderating role of globalization," *Energy Policy*, vol. 202, p. 114554, 2025, https://doi.org/10.1016/j.enpol.2025.114554.

[10] F. Eze, M. Egbo, U. J. Anuta, O.-B. R. Ntiriwaa, J. Ogola, and J. Mwabora, "A review on solar water heating technology: Impacts of parameters and techno-economic studies," *Bull. Natl. Res. Cent.*, vol. 48, no. 1, Mar. 2024, https://doi.org/10.1186/s42269-024-01187-1.

[11] F. Al Mubarak, R. Rezaee, and D. A. Wood, "Economic, societal, and environmental impacts of available energy sources: A review," *Eng*, vol. 5, no. 3, pp. 1232–1265, 2024.

[12] A. Remlaoui *et al.*, "Numerical simulation of a forced circulation solar water heating system," *Sci. Rep.*, vol. 14, no. 1, p. 28999, 2024.

[13] S. Ma, S. Li, Q. Luo, Z. Yu, and Y. Wang, "Revisiting the relationships between energy consumption, economic development and urban size: A global perspective using remote sensing data," *Heliyon*, vol. 10, no. 5, p. e27318, 2024, https://doi.org/10.1016/j.heliyon.2024.e27318.

[14] Y. Krozer, S. Bykuc, and F. Coenen, "Growth of Renewable Energy: A Review of Drivers from the Economic Perspective," *Energies (Basel).*, vol. 18, no. 19, p. 5250, 2025.

[15] M. A. Polat, "The impact of transition from fossil fuels to renewable energy on carbon emissions: The case of the European Union," *International Journal of Energy Studies*, vol. 10, no. 3, pp. 909–927, 2025.

[16] M. Y. Raza and B. Lin, "Renewable energy substitution and energy technology impact in a transitional economy: A perspective from Pakistan," *J. Clean. Prod.*, vol. 360, p. 132163, 2022, https://doi.org/10.1016/j.jclepro.2022.132163.

[17] S. Jaisankar, J. Ananth, and K. N. Sheeba, "Advances in thermal solar water systems for efficient and sustainable energy conversion: An extensive review of design, experimentation, simulation and optimization," *Renewable and Sustainable Energy Reviews*, vol. 226, p. 116449, 2026.

[18] F. Eze, M. Egbo, U. J. Anuta, O.-B. R. Ntiriwaa, J. Ogola, and J. Mwabora, "A review on solar water heating technology: Impacts of parameters and techno-economic studies," *Bull. Natl. Res. Cent.*, vol. 48, no. 1, p. 29, 2024.

[19] M. Khaleel, Z. Yusupov, A. Ahmed, A. Alsharif, Y. Nassar, and H. El-Khozondar, "Towards sustainable renewable energy," *Applied solar energy*, vol. 59, no. 4, pp. 557–567, 2023.

[20] S. A. Kalogirou, *Solar energy engineering: processes and systems*. Elsevier, 2023.

[21] B. Ramlow and B. Nusz, *Solar water heating: a comprehensive guide to solar water and space heating systems*. New Society Publishers, 2023.

[22] I. Meireles, V. Sousa, B. Bleys, and B. Poncelet, "Domestic hot water consumption pattern: Relation with total water consumption and air temperature," *Renewable and Sustainable Energy Reviews*, vol. 157, p. 112035, 2022.

[23] Y. A. Selikhov, V. A. Kotsarenko, J. J. Klemeš, and P. O. Kapustenko, "The performance of plastic solar collector as part of two contours solar unit," *Chem. Eng. Trans*, vol. 70, 2018.

[24] M. Järvinen *et al.*, "Solar Energy," in *Designing Renewable Energy Systems within Planetary Boundaries: A Textbook for Energy Engineers*, M. Järvinen and H. Paulomäki, Eds., Cham: Springer Nature Switzerland, 2025, pp. 247–344. https://doi.org/10.1007/978-3-031-69856-9_4.

[25] Z. Rahimi-Ahar, M. Khiadani, L. Rahimi Ahar, and A. Shafieian, "Performance evaluation of single stand and hybrid solar water heaters: a comprehensive review," *Clean Technol. Environ. Policy*, vol. 25, no. 7, pp. 2157–2184, 2023.

[26] O. Adetifa Babatunde, D. Salami Wasiu, M. Samuel Taiwo, A. Babalola Ayoola, and O. Sosanya Abolade, "Adapting Television Satellite Dish for Low-Temperature Solar Thermal Application: Experimental Evaluation".

[27] T. V Kadam, S. Y. Pakhare, and A. B. Godse, "'Performance analysis of solar thermal collectors: A comprehensive review,'" *Measurement: Energy*, vol. 7, p. 100059, 2025. https://doi.org/10.1016/j.meaene.2025.100059.

[28] C. Gao, J. Hu, S. Zhao, J. Wang, Y. Fu, and W. Wang, "Systematic Review on the Heat Transfer Optimization of Solar Collectors," Dec. 01, 2025, *Springer*. https://doi.org/10.1007/s10765-025-03649-8.

[29] W. L. Al-Salim, J. M. Al -Asadi, and M. A. Mahdi, "Effect of Carbon Nanoparticles on the Performance Efficiency of a Solar Water Heater," *Iraqi Journal of Physics*, vol. 20, no. 1, pp. 82–92, 2022, https://doi.org/10.30723/ijp. v20i1.97.

[30] "THE EFFECT OF REFLECTOR SHAPE ON THE PERFORMANCE OF SOLAR COLLECTORS," *MINAR International Journal of Applied Sciences and Technology*, vol. 07, no. 03, Sep. 2025, https://doi.org/10.47832/2717-8234.24.17.

[31] Y. Kumar, M. Verma, H. K. Ghritlahre, and P. Verma, "Recent Developments in the Thermal Performance of Flat Plate Solar Water Heaters with Reflectors-A Review," 2022, *Taylor and Francis Ltd.* https://doi.org/10.1080/15567036.2022.2131940.

[32] M. RÖNNELID and B. KARLSSON, "THE USE OF CORRUGATED BOOSTER REFLECTORS FOR SOLAR COLLECTOR FIELDS," *Solar Energy*, vol. 65, no. 6, pp. 343–351, 1999, doi: https://doi.org/10.1016/S0038-092X(99)00009-2.

[33] N. Saraswat, M. Pandeya, R. K. Pareek, and K. S. Kulhar, "Solar Energy in Developing Countries: Challenges and Opportunities for Smart Cities," in *E3S Web of Conferences*, EDP Sciences, Jun. 2024. https://doi.org/10.1051/e3sconf/202454004003.

[34] S. K. Teklemariam, R. Schiasselloni, L. Cattani, and F. Bozzoli, "Solar Energy Solutions for Healthcare in Rural Areas of Developing Countries: Technologies, Challenges, and Opportunities," Aug. 01, 2025, *Multidisciplinary Digital Publishing Institute (MDPI)*. https://doi.org/10.3390/en18153908.

[35] D. Wei *et al.*, "Optimum tilt and azimuth angles of heat pipe solar collector, an experimental approach," *Case Studies in Thermal Engineering*, vol. 55, Mar. 2024, https://doi.org/10.1016/j.csite.2024.104083.

[36] A. K. Mohammed, I. A. Hamakhan, and R. B. Weli, "Effect of Collector Tilt Angle on the Performance of Solar Water Heating System in Erbil of Iraq," *Int. J. Heat Technol*, vol. 40, pp. 1293–1298, 2022.

[37] M. Jenčo, "Determination of the Solar Angle of Incidence Using an Equivalent Surface and the Possibility of Applying This Approach in Geosciences and Engineering," *ISPRS Int. J. Geoinf.*, vol. 14, no. 9, Sep. 2025, https://doi.org/10.3390/ijgi14090323.

[38] S. A. Kalogirou, *Solar energy engineering: processes and systems*. Elsevier, 2023.

[39] M. A. Saleh, S. Kaseb, and M. F. El-Refaie, "Glass–azimuth modification to reform direct solar heat gain," *Build. Environ.*, vol. 39, no. 6, pp. 653–659, 2004.

[40] A. Zerrouki, A. Boumédien, and K. Bouhadef, "The natural circulation solar water heater model with linear temperature distribution," *Renew. Energy*, vol. 26, no. 4, pp. 549–559, 2002, https://doi.org/10.1016/S0960-1481(01)00146-X.

[41] T. T. Chow, W. He, and J. Ji, "Hybrid photovoltaic-thermosyphon water heating system for residential application," *Solar Energy*, vol. 80, no. 3, pp. 298–306, 2006, https://doi.org/10.1016/j.solener.2005.02.003.

[42] R. D. Salim, "Manufacturing procedure of a hybrid design of solar collector (sterilization and water heating) by solar and electrical energy," in *2018 International Conference on Advanced Science and Engineering (ICOASE)*, IEEE, 2018, pp. 353–356.

[43] P. Pissavi, "Modelling of the dynamic behavior of a tank for solar storage with internal exchanger," *Re´ v Ge´ n Thermique*, pp. 246–247, 1982.

[44] A. S. Abdulsitar and N. A. Hasan, "Comparison between spiral and serpentine flow solar water heater," *Journal of University of Babylon for Engineering Sciences*, pp. 89–99, 2022.

[45] I. Bendjamaa, T. Allaoui, Y. Menni, A. J. Chamkha, and G. Lorenzini, "Study and Comparison Between Two Receivers of Parabolic Trough Collector.," *Mathematical Modelling of Engineering Problems*, vol. 6, no. 3, 2019.

[46] S. M. Saleh and M. M. M. Alaskari , "Parametric Study of Active Solar Heating Using a Pebble Bed as a Thermal Collector and Storage Unit," 2014.

[47] W. Ariyawiriyanan *et al.*, "Thermal efficiency of solar collector made from thermoplastics," *Energy Procedia*, vol. 34, pp. 500–505, 2013.

[48] J. A. Aldhaibani, A. Yahya, and R. B. Ahmad, "Optimizing power and mitigating interference in LTE-A cellular networks through optimum relay location," *Elektron. Ir Elektrotech.*, vol. 20, no. 7, 2014.

[49] M. Abbas and I. M. Ahmed, "A review of secure and efficient data transmission in IoT systems: Advances and open research challenges," *Journal of Telecommunication and Computer Technology*, vol. 1, no. 1, pp. 1–20, 2026.

[50] S. F. Abdul-Razzaq, R. S. E.-D. Sabah, and A.-J. F. Abdul-Razzaq, "Microstrip antenna for non-invasive glucose sensing using FR-4 substrate material," Interdisciplinary Journal of Health, Environment and Computation, vol. 1, no. 3, pp. 23–35, Jan.–Mar. 2026. [Online]. Available: https://doi.org/10.65983/ijhec.2026.03.0003.